New solid solvates of C60 and C70 fullerenes: The relationship between structures and lattice energies

ARTICLE *in* CARBON · JANUARY 2003

Impact Factor: 6.2 · DOI: 10.1016/S0008-6223(03)00379-8

PERGAMON

Carbon 41 (2003) 2743–2755

CARBON

New solid solvates of C_{60} and C_{70} fullerenes: The relationship between structures and lattice energies

Mikhail V. Korobov[a,*], Evgeny B. Stukalin[a], Andrey L. Mirakyan[a], Ivan S. Neretin[b], Yuri L. Slovokhotov[b], Alexender V. Dzyabchenko[c], Aleksey I. Ancharov[d], Boris P. Tolochko[d]

[a]*Chemistry Department, Moscow State University, Lenmins Hills 1, 119992 Moscow, Russia*
[b]*Institute of Organoelement Compounds R.A.S., Moscow, Russia*
[c]*Institute of Nuclear Physics, Novosibirsk, Russia*
[d]*Karpov Institute of Physical Chemistry, 10 Vorontsovo Pole, 103064 Moscow, Russia*

Received 18 June 2003; accepted 5 August 2003

Abstract

The goal of this study was to establish the relationship between the X-ray and the thermodynamic data on fullerene's solvated crystals. X-ray diffraction study of 12 solid solvates of C_{60} and C_{70} with different aromatic solvents have been performed. It has been demonstrated that the solid solvates under consideration were typical van-der-Waals complexes with the negative excess volumes, packing coefficients from 0.72 to 0.78, stable due to the formation of the fullerene to solvent bonds, reasonably described by six to 12 Lennard–Jones potentials. The atom–atom potential method has been used to describe both the crystal structures and the thermodynamics of the solid solvates. The minimization of the lattice energy with respect to the cell and rigid body parameters ($T=0$ K) has led to the crystal structures very close to the experimental ones. The minimum energies found have reasonably reproduced the calorimetric lattice energies of the solvates. The theory has also demonstrated its ability to account for the trends in thermodynamic stability of solid solvates, e.g., has predicted correctly the low stability of the hypothetical monoclinic solvate $C_{60}\cdot 2C_6H_{14}$.

Keywords: A. Fullerene; C. Crystal structure; Modeling; D. X-ray diffraction; Thermodynamic properties

1. Introduction

C_{60} and C_{70} fullerenes form solid solvates with almost all commonly used solvents. The solubility of fullerenes, which is of great importance for their purification and chemical reactivity, is strongly affected by the formation of these van der Waals complexes. Solvates are responsible for the unusual temperature dependence of fullerene's solubility [1]. Formation of the solvates could hinder the disorder in the C_{60} sublattice and bring the C_{60} spheres closer to each other. This makes some solvates promising precursors for the synthesis of the fullerene's dimers [2].

The composition and stability of the solvates are closely related to their crystal structures. However, single crystal X-rays diffraction studies are often hindered by the low quality of the crystals. Only a few structures have been studied to date, namely: solvates of C_{60} with benzene [3,4], *m*-xylene [5] and solvate of C_{70} with *m*-xylene [6]. In addition, solvates of C_{60} with pentane [7] and trichloroethylene [8], and of C_{70} with benzene [9] and toluene [10] were studied by powder XRD.

This work reports on the single-crystal determinations of five new fullerene solvates: $C_{60}\cdot 2C_6H_5Me$ (**1a**), $C_{60}\cdot 2C_6H_5I$ (**2**), $C_{60}\cdot 3o\text{-}C_6H_4Br_2$ (**3**), $C_{60}\cdot 2m\text{-}C_6H_4Br_2$ (**4a**), and $C_{70}\cdot 2o\text{-}C_6H_4Me_2$ (**5**). Incomplete single-crystal data were obtained for $C_{60}\cdot C_6H_5Me$ (**1b**). The powder XRD study resulting in cell dimensions was performed for $C_{60}\cdot C_6H_5Cl$ (**6**), $C_{60}\cdot 2o\text{-}C_6H_4Me_2$ (**7**), $C_{60}\cdot 2/3m\text{-}C_6H_4Br_2$ (**4b**), $C_{60}\cdot 2/3m\text{-}C_6H_5Me_2$ (**8**), $C_{60}\cdot 2/3m\text{-}C_6H_4Cl_2$ (**9**) and $C_{60}\cdot 2/3(1,3,5\text{-}C_6H_3Me_3)$ (**10**) where Me stands for

*Corresponding author. Tel.: +7-95-393-1578; fax: +7-95-932-8846.

E-mail address: korobov@phys.chem.msu.ru (M.V. Korobov).

0008-6223/03/$ – see front matter
doi:10.1016/S0008-6223(03)00379-8

CH_3. The new structures and those available from the literature are discussed in comparison with experimental thermochemical data namely lattice energies of the solvates calculated using non-bonded atom–atom potentials are compared with the lattice energies estimated from calorimetric measurements. In this way we attempt to account for trends observed in the relative thermal stability of the solvates. The experimental crystal structures on the other hand are compared with the ones simulated by minimization of lattice energy at $T=0$ K.

2. Experimental part

2.1. Preparation of the solvates

Samples of C_{60} were obtained from Bucky, USA (99.5 mol% purity) and Fullerene Technologies, St. Petersburg, Russia (99.9% mol purity). C_{70} were from MER (>99% mol purity). The solvents *o*- and *m*-dibromobenzene of 98 and 97% purity, respectively, were from Lancaster. All other solvents used had the trademark HP and were distilled twice before use.

Solvates **2, 3, 4a, 5–7** and **10** are solid phases in equilibrium with the corresponding saturated solutions at $T=298$ K. They were obtained by precipitation from the initially undersaturated solutions. Saturated solutions of C_{60} and C_{70} in corresponding solvents were dried slightly under low vacuum and were left to stand at room temperature until the precipitation started. Crystals for the X-ray measurements were then carefully taken from the mother liquor. The solid phase precipitated from a saturated solution of C_{60} in toluene consisted of a mixture of **1a** and **1b**. Samples for the X-ray study of both **1a** and **1b** were extracted from this mixture. Solvates **4b, 8** and **9** were obtained by heating of **4a**, $C_{60}\cdot(2.3–3.6)m\text{-}C_6H_5Me_2$ and of $C_{60}\cdot\{2.3\pm0.5\}m\text{-}C_6H_4Cl_2$, respectively, above their incongruent melting points [1]. The solid solvates formed were identified by means of the differential scanning calorimetry (DSC). A DSC-30 Mettler instrument was used to capture DSC traces. The DSC identification of the solvates was based on the measured temperatures and enthalpies of the incongruent melting. The compositions of the solvates were also determined, using the DSC procedure previously described in the literature [1,11].

2.2. X-ray experiments

Parameters of the X-ray experiments are listed in the Table 1. All structures were solved with direct methods and refined with full-matrix least squares on F2 using SHELXTL program package [12]. Hydrogen atoms were placed in geometrically calculated positions and refined within the 'riding atom' model. In **1a**–**4a** all non-hydrogen atoms were refined in anisotropic approximation. Although the unit cell of compound **3** is close to hexagonal ($a\approx c$, $\beta\approx120°$), the molecular arrangement does not reveal the hexagonal pseudosymmetry. For one of the two disordered solvent molecules, only the bromine atoms positions of the minor component were revealed.

Unit cell parameters for **1b** were derived from incomplete single crystal data and for **4b, 6, 7, 8** and **10**− from the powder XRD data. Indexing of powder patterns and refinement of unit cell parameters were performed using the TREOR [13] and PIRUM programs. Final cell data parameters are listed in the Table 2.

2.3. Lattice energy calculations.

The atom–atom potential method [14] provides a useful tool to assess and to understand various structural and calorimetric experimental observations based on both thermodynamic grounds (minimum-free energy condition at $T=0$ K imposed on the geometric structure) and on reasonable assumptions regarding molecular geometry. Intermolecular potential are postulated to be a sum of pairwise interatomic potential functions. The PMC program [15,16] was used to calculate the lattice energies of the solvate structures and to perform the minimization of lattice energies with respect to the lattice constants and rigid-body parameters of the fullerenes and the solvent molecules. The van der Waals energy was described as a sum of atom–atom Lennard–Jones-type (6–12) potentials

$$V(r) = e[2(r_0/r)^6 - (r_0/r)^{12}]$$

with the parameters e and r_0 summarized in Table 3.

The C···C parameters of this table have been proved successful in the prediction of the lattice energies and equilibrium structures of C_{60} [15] and C_{70} [18]. The other potentials (involving the H, Cl, and Br atoms) have been compiled on the basis of previous theoretical work on the crystal structure predictions of hydrocarbons [19] and tested on a number of test compounds with respect to their ability to reproduce known crystal structures and sublimation enthalpies (Dzyabchenko, A.V., unpublished results, 2001). The total intermolecular potential used previously with pure C_{60} also involves an electrostatic term that provided about 10% of the total energy [15]. In the context of present work, however, this term was recognized to be less significant and ignored throughout the calculations.

3. Results and discussion

3.1. Structural properties

X-ray single crystal studies of the five new compounds were performed. High degree of disorder in **1a**, **3** and **5** gives rise to high R values. However, unit cell parameters allowing correlations of thermochemical data with crystallography were obtained, and the molecular arrangement

Table 1
Parameters of single crystal X-ray experiments

Compound	**1a**	**2**	**3**	**4a**	**5**
Composition	$C_{60}\cdot 2C_6H_5CH_3$	$C_{60}\cdot 2PhI$	$C_{60}\cdot 3m\text{-}C_6H_4Br_2$	$C_{60}\cdot 2m\text{-}C_6H_4Br_2$	$C_{70}\cdot 2o\text{-}C_6H_4(CH_3)_2$
Max. 2θ (°)	50.1	60	60	60	44.18
Lattice	Monoclinic	Monoclinic	Monoclinic	Monoclinic	Triclinic
Space group	*C2/m*	*C2/c*	$P2_1/c$	*C2/m*	*P-1*
Site symmetry:					
Fullerene	2/*m*	−1	1	2/*m*	1
Solvent	*M*	1	all 1	*M*	both 1
a (Å)	17.03(2)	24.185(3)	12.946(8)	13.149(4)	11.162(8)
b (Å)	10.344(4)	9.889(1)	30.496(18)	15.285(5)	11.201(8)
c (Å)	11.16(1)	17.462(2)	13.253(8)	9.872(3)	19.01(2)
α (°)	90	90	90	90	89.46(7)
β (°)	107.10(7)	113.724(4)	117.35(1)	91.59(4)	78.66(6)
γ (°)	90	90	90	90	73.36(4)
V (Å^3)	1879	3815	4648	1983	2230
Z	2	4	4	2	2
F(000)	920	2192	2760	1160	1072
ρ_{calc} (g/cm^3)	1.599	1.965	2.04	1.997	1.568
μ (mm^{-1})	0.09	1.71	5.26	4.12	0.09
X-ray device	Siemens P3			Bruker SMART	Siemens P3
T (K)	150	110	110	110	150
X-ray wavelength	Mo Kα	Mo Kα	Mo Kα	Mo Kα	Mo Kα
Reflections	2360	15905	39348	8487	4168
Independent	1761	5482	13625	2973	3835
Observed ($F>4\sigma$)	1148	4467	4766	2553	2179
Parameters refined	176	334	681	188	425
R ($F>4\sigma$)	0.226	0.0302	0.15	0.029	0.251
WR_2	0.641	0.0877	0.316	0.079	0.666
G.O.F.	1.064	1.025	1.063	1.047	1.039

is objectively revealed in all cases (see Table 1). Unit cell parameters for another seven solvates were derived using powder XRD and for **1b-** using incomplete single crystal data (see Table 2).

Monoclinic toluene solvate **1a** is isostructural to the previously known bromobenzene analogue of the same C_{60} to solvent composition [20]. The iodobenzene solvate **2**, although of a different space group and positional symme-

Table 2
Unit cell parameters derived from powder or incomplete single crystal XRD

	1b	**6**	**7**	**4b**	**8**	**9**	**10**
Solvate	$C_{60}\cdot C_6H_5Me$	$C_{60}\cdot C_6H_5Cl$	$C_{60}\cdot 2$ (o-$C_6H_4Me_2$)	$C_{60}\cdot 2/3$ (m-$C_6H_4Br_2$)	$C_{60}\cdot 2/3$ (m-$C_6H_4Me_2$)	$C_{60}\cdot 2/3$ (m-$C_6H_4Cl_2$)	$C_{60}\cdot 2/3$ ($C_6H_3Me_3$)
X-ray device	Siemens P3	DRON	DRON	DRON	DRON	SSRC	SSRC
Method	Single cryst.			Powder XRD			
T (K)	150	298	298	298	298	298	298
X-ray wavelength	Mo Kα	Cu Kα	Cu Kα	Cu Kα	Cu Kα	Cu Kα	Cu Kα
Lattice	Monoclinic	Monoclinic	Monoclinic	Hexagonal	Hexagonal	Hexagonal	Hexagonal
A (Å)	10.25(3)	10.23(1)	15.33 (1)	23.86(2)	23.786(7)	23.8098(9)	23.742(1)
B (Å)	31.3(1)	31.69(2)	13.08 (4)	23.86(2)	23.786(7)	23.8098(9)	23.742(1)
C (Å)	10.17(4)	10.06(2)	10.01 (3)	10.11(1)	10.15(2)	10.130(1)	10.167(1)
α (°)	90	90	90	90	90	90	90
β (°)	94.0(3)	93.2 (1)	99.4 (1)	90	90	90	90
γ (°)	90	90	90	120	120	120	120
V (Å^3)	3255	3256	1980	4985	4973	4973	4963
Z	4	4	2	6	6	6	6

Table 3
Parameters of the (6–12) atom–atom potentials

Atoms	r_0 (m^{-10})	$-e$ (kJ/mol)	Refs.
H···H	2.93	0.150	[17]
H···C	3.32	0.196	[17]
C···C	3.70	0.301	[17]
Cl···Cl	4.00	1.200	Dzyabchenko A.V., unpublished results 2001
H···Cl	3.40	0.418	Dzyabchenko A.V., unpublished results 2001
C···Cl	3.70	0.698	Dzyabchenko A.V., unpublished results 2001
Br···Br	4.00	2.090	Dzyabchenko A.V., unpublished results 2001
H···Br	3.47	0.418	Dzyabchenko A.V., unpublished results 2001
C···Br	3.85	0.836	Dzyabchenko A.V., unpublished results 2001

try, is similar to both of them in molecular arrangement. Their unit-cell vectors are in the obvious relationships: **a**(**2**)≈2**c**(**1**)–**a**(**1**), **b**(**2**) ≈–b(**1**), **c**(**2**)≈a(**1**).

Fullerene spheres are arranged in distorted hexagonal layers with solvent molecules in trigonal prismatic cavities between layers (Fig. 1). Each C_{60} has six closest neighboring C_{60} molecules in the same layer at the distances $d=10.4$ Å, while the distances between layers are greater than 11 Å. Similar arrangement of C_{60} molecules was observed in the binary $C_{60}\cdot 2Cp_2Fe$ [21] and ternary $C_{60}\cdot(2-x)S_4N_4\cdot xC_6H_6$ [22]. molecular complexes. Analogous fullerene packing motifs with perfect hexagonal symmetry was revealed in a family of solvates of C_{60} with CCl_4 [23,24], $CHCl_3$, CH_2Cl_2, $CHBr_3$ [24] and in a molecular complex with P_4 [25]. Geometrical parameters of fullerene packing are listed in Table 4. It is interesting that the $C_{60}\cdot 2S_8$ complex with a similar 1:2 composition has a different packing motif [26].

The unit cell of iodobenzene solvate is twice as large as those of two other solvates. The relation of the respective unit cells and symmetry elements is shown on Fig. 1. In bromobenzene and toluene solvates, C_{60} molecules are located in special positions of $2/m$ symmetry while solvent molecules lie on the mirror planes perpendicular to them. In the iodobenzene solvate, where site symmetry is lower, the fullerene molecule is located in the inversion center and solvate molecules are in general positions.

The closest contacts between fullerene molecules along 010 are between the pairs of C atoms linked by the 6,6 bond. In $C_{60}\cdot 2C_6H_5Br$, the corresponding bonds of neighboring molecules are brought together (Fig. 2a), and C···

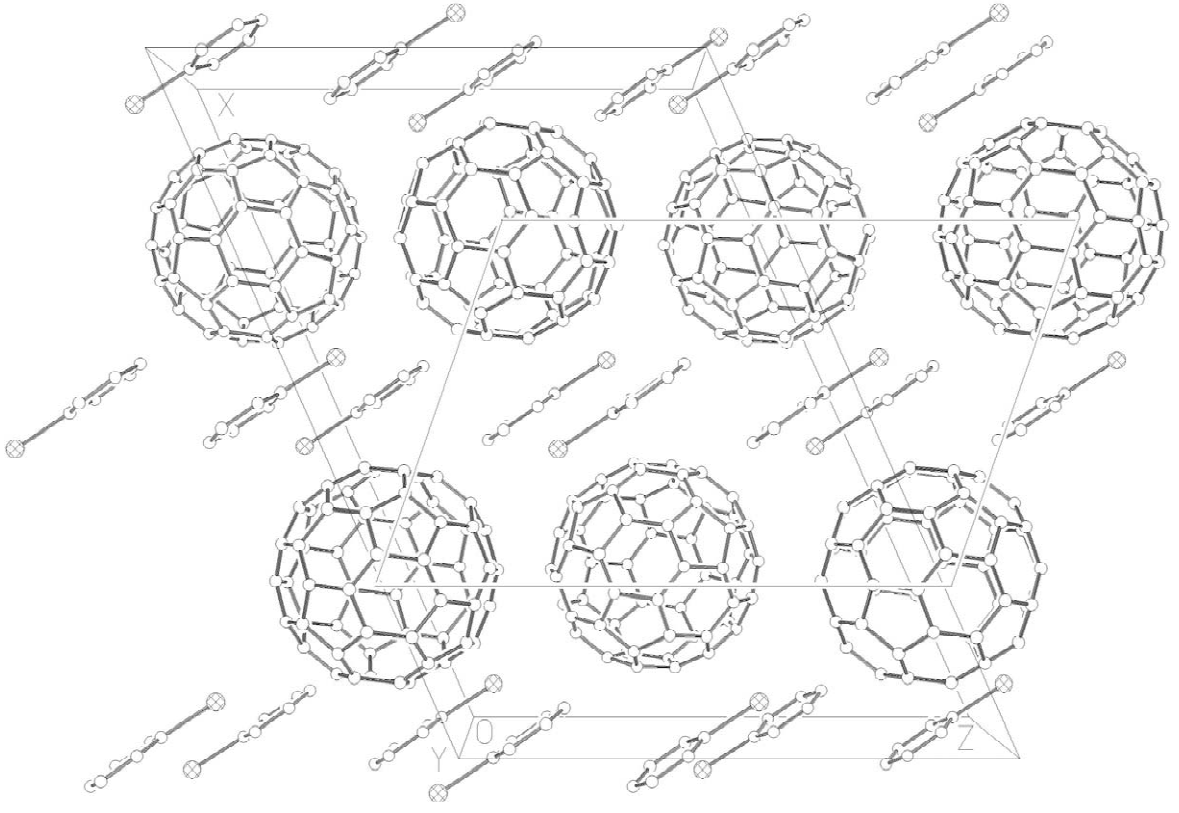

Fig. 1. Molecular packing in C_{60}:iodobenzene solvate **2**. Unit cell of the isostructural bromobenzene solvate is shown in single lines.

Table 4
Geometrical parameters of C_{60} molecules packing in 1:2 solvates

Compound	$C_{60}\cdots C_{60}$ in the layer (Å)	Average	$C_{60}\cdots C_{60}$ between layers	Layer-to-layer	Refs.
$C_{60}\cdot 2PhMe$	9.96×4, 10.34×2	10.09	11.16	10.67	This work
$C_{60}\cdot 2PhBr$	10.00×4, 10.16×2	10.06	11.34	10.78	[20]
$C_{60}\cdot 2PhI$	10.02×4, 9.89×2	9.98	11.72	11.07	This work
$C_{60}\cdot 2CCl_4$	10.10×6	10.10	10.75	10.75	[23]
$C_{60}\cdot 2CHCl_3$	10.08×6	10.08	10.11	10.11	[24]
$C_{60}\cdot 2CHBr_3$	10.21×6	10.21	10.21	10.21	[24]
$C_{60}\cdot 2P_4$	10.08×6	10.08	10.10	10.10	[25]
$C_{60}\cdot 2Cp_2Fe$	9.90×2, 10.37×2, 10.40×2	10.22	11.34	11.26	[21]
$C_{60}\cdot(2-x)\ S_4N_4\cdot xC_6H_6$	9.87–10.06	9.92	9.92	11.01	[22]

C distance is 3.22 Å. In **1a**, the contacting fullerene molecules are in different orientation to each other, therefore the closest C···C distances (3.24 Å) are almost similar to those in the bromobenzene solvate, whereas the center-to-center separation is significantly lower (9.89 Å instead of 10.16 Å in the bromobenzene solvate) (Fig. 2b). Four other contacts within the layer are formed by the two atoms of the 6,6 bond from one molecule and the hexagonal face of the other one and have larger interatomic separations (3.4–3.6 Å).

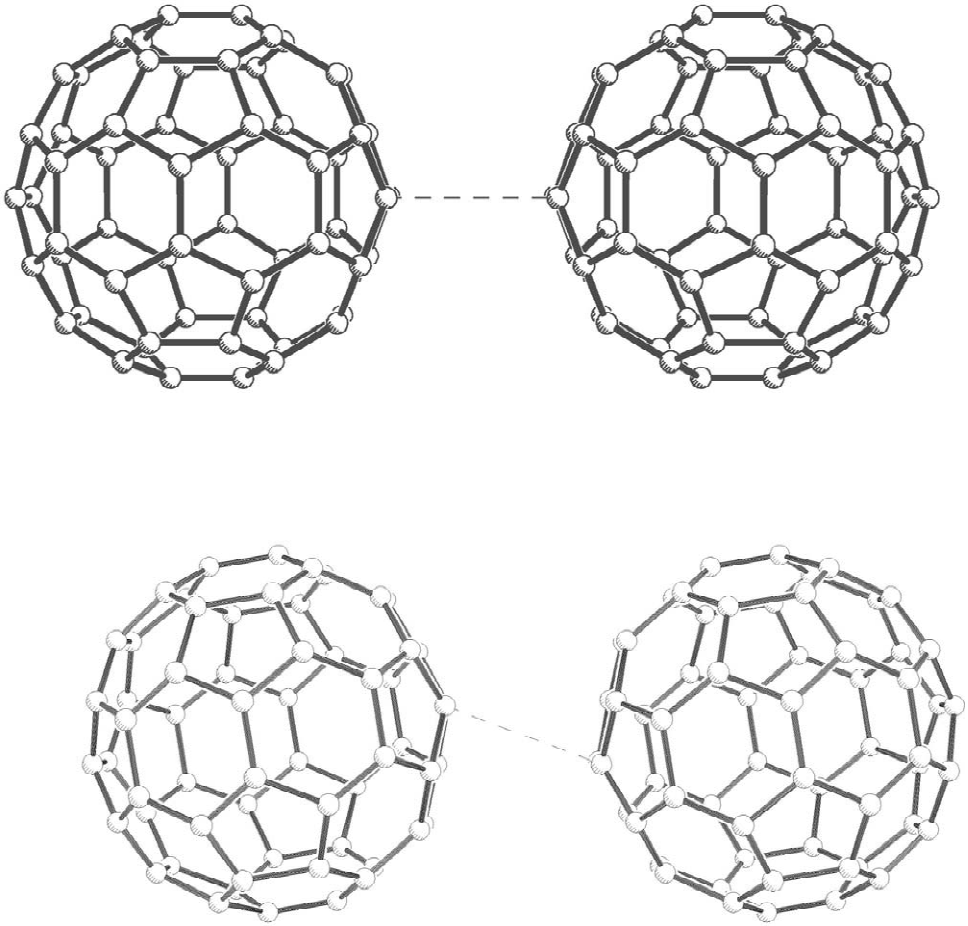

Fig. 2. Nearest $C_{60}\cdots C_{60}$ contacts in the bromobenzene (a) and iodobenzene (b) solvates.

Halogen atom of the solvent molecule heads to the one of fullerene's carbon atoms at the distance 3.23 Å for bromine [20] and 3.31 Å for iodine. For comparison, related compounds $C_{60}\cdot C_6H_6\cdot CH_2I_2$ [27] and $C_{60}\cdot C_6H_5CH_3\cdot I_2$ [28] contain C···I contacts of 3.29 and 3.09 Å, respectively.

C_{60} and toluene form another solvate of composition 1:1, possibly metastable at all temperatures [1]. Incomplete single crystal X-ray diffraction data for **1b** revealed a monoclinic unit cell with parameters close to those of chlorobenzene solvate **6**. Although the molecular arrangement could not be derived from our data, it may be proposed that the fullerene packing motif is similar to that in orthorhombic solvates with pentane [7] and trichloroethylene [8], since their unit cell dimensions are near to those of **1b** and **6**.

The solvate **3**, in contrast with the all other compounds studied, has a 1:3 composition. Two of the three independent solvent molecules are disordered, whereas the C_{60} moiety is well-ordered. The packing of fullerene molecules shows a diamond-like framework (Fig. 3). Other types of low-density $(C_{60})_n$ frameworks have been ob-

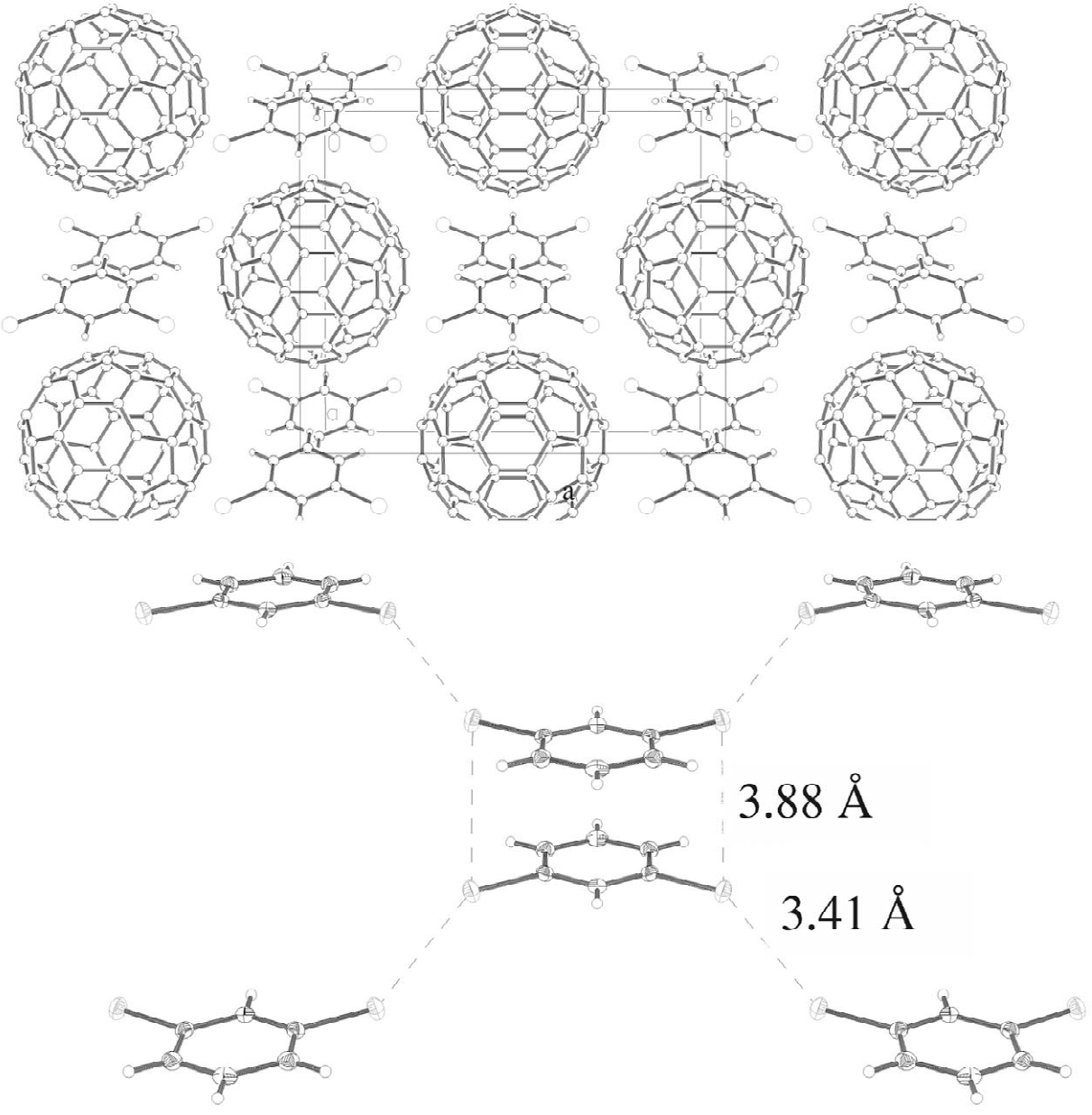

Fig. 3. Molecular packing in **3** (a) and aggregate of solvent molecules (b).

served earlier in the benzene solvate $C_{60}\cdot 4C_6H_6$ [3,4] and the molecular complex $C_{60}\cdot 2S_8$ [26]. The distances between C_{60} centers in this framework are listed in the Table 5. Shortened C···C contacts are absent, while bromine atoms have very short Br···Br contacts down to 3.50 Å, sticking solvent molecules together into zigzag chains.

In the fully ordered structure of **4** with composition 1:2 (**4a**), C_{60} spheres form a distorted simple cubic arrangement, while the pairs of stacked solvent molecules are located in the cavities (Fig. 4). A very short contacts between bromine atoms (down to 3.40 Å) join the solvent molecules into a 3D framework. Shortest C···C contacts between the fullerene molecules have a length of 3.31 Å, which is normal for van der Waals contact. At higher temperature (336 K [11]), **4a** transforms to another solvate (**4b**) with lower solvent to fullerene ratio. According to the XRD study, it belongs to a family of isomorphous hexagonal solvates alongside with **7**, **8** and **9**. Earlier a single crystal X-ray study by Ramm et al. [5] reported a composition of 1:2 for **7**. However, very short intermolecular contacts in this structure indicate a possible error in composition due to extensive disorder of the solvent molecules. Space-filling considerations together with DSC data yield in a molar ratio of 1:2/3, i.e., 2/3 solvent molecules per one C_{60} molecule.

The crystal structure of $C_{70}\cdot 2o\text{-}C_6H_4Me_2$ contains puckered layers of C_{70} molecules with *o*-xylene molecules in the cavities (Fig. 5). Fullerene and two independent solvent molecules are in general positions. The long axes of the C_{70} molecules are inclined at 70° relative to the layers. The C_{70} molecule is orientationally disordered, but the details of the disorder could not be revealed due to the lack of measured reflections.

3.2. Thermodynamic properties

Table 6 summarizes the thermodynamic properties, packing coefficients (*k*), dilution parameters (*d*), changes of volume for some solvated crystals of C_{60} and C_{70} with the aromatic solvents, alkanes and CCl_4.

It was once claimed, that, contrary to solvates with alkanes, the solvated crystals of C_{60} with the aromatic solvents are formed with positive excess volume [29]. This statement was based on the single example of the $C_{60}\cdot 4C_6H_6$ solvate, formed from C_{60} and the high pressure monoclinic phase of benzene. X-ray data obtained in the present study (Table 6) has proved, that the excess volume is negative both for the formation of the solvate by reaction of fullerene with the liquid

$$C_n(s) + rS(liq) = C_n \cdot rS(s) \quad (1)$$

and solid solvent

$$C_n(s) + rS(s) = C_n \cdot rS(s) \quad (2)$$

where $n = 60$ or 70.

Data for reaction (2) are presented only in a few cases, since data on molar volumes of the solvents in the solid state are limited.

The negative excess volumes and packing coefficients are even slightly higher for the 'aromatic solvates' compared to the 'solvates with alkanes' (columns II and III, respectively, in Table 6). The thermodynamic properties of two groups of solvates are significantly different. The most informative is the comparison of the entropies and enthalpies of the reaction (1) with the entropies and enthalpies of melting of the pure solvents, respectively (columns IV and V in Table 6).

Formation of solvates of C_{60} with arenes causes 'ordering', i.e., significant loss of the entropy and of the enthalpy. The typical entropy of the reaction (1) per mole of a solvent is below -50 J/mol K, which is comparable or more negative than the entropy of freezing of pure arenes (see Table 6). Contrary to the behavior of solvates with arenas, solvates with alkanes are relatively 'less ordered', 'clathrate-type' compounds. The entropy and the enthalpy of the reaction (1) are less negative than the corresponding values for the solvent freezing. The chemical identity of the solvents is less pronounced. The same simple composition (1:1) is formed in all cases

It is worth noting, that the dilution parameter (*d*),

$$d = \{V_{cell} - V(C_{60})\}/V(C_{60}),$$

[32]; where V_{cell}, $V(C_{60}) = 525$ Å^3 are the unit cell volume of the solvate per formula unit and the van der Waals molar volume of C_{60}, respectively, is nearly constant for certain types of a solvate, e.g., for the whole family of (1:2) monoclinic solvates it is equal to 0.83, though the group includes both relatively stable solvate with iodoben-

Table 5
Parameters of diamond-like fullerene packing in molecular complexes

Compound	Shortest $C_{60}\cdots C_{60}$ distances	Average	Next shortest $C_{60}\cdots C_{60}$	Refs.
$C_{60}\cdot 3o\text{-}C_6H_4Br_2$	10.01×2, 10.05, 10.14	10.05	12.95	This work
$C_{60}\cdot 4C_6H_6$	9.94×2, 9.95, 9.99, 10.07, 10.34	10.04	12.74	[4]
$C_{60}\cdot 2S_8$	10.04×2, 10.10×2, 10.54×2	10.23	13.44	[26]

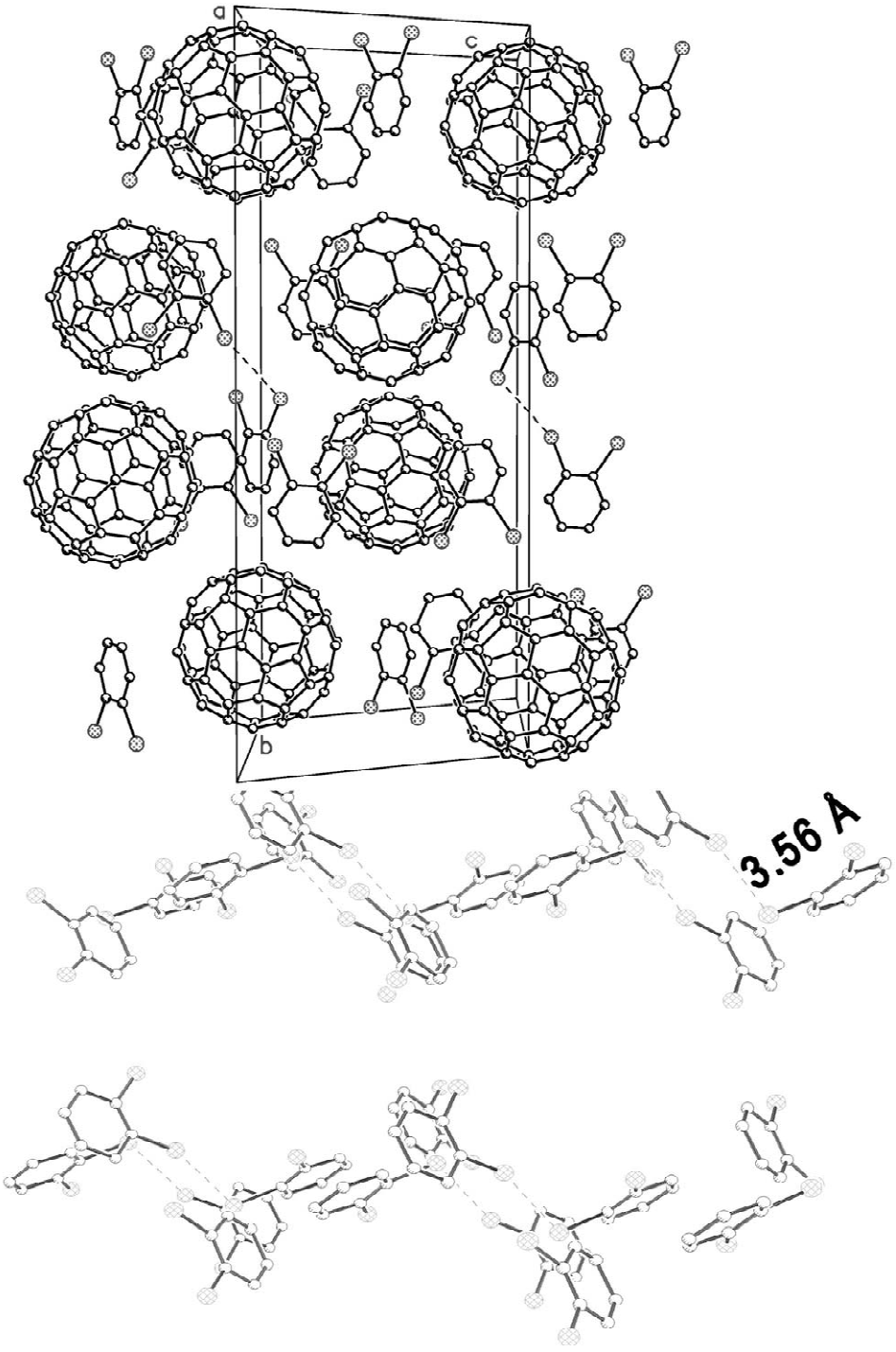

Fig. 4. Molecular packing in **4a** (a) and solvent molecules aggregate (b).

zene and relatively unstable one with CCl_4. The dilution parameter changes significantly while going from one family of the solvates to another. One may speculate that the solvates in question are host-quest complexes with nearly fixed amount of the empty space (d = constant), available for the solvent molecules, characteristic for every lattice. Alkanes do not form $C_{60}\cdot 2S$ crystals. The molecular arrangement presented in Fig. 1 for the solvates (1:2) of

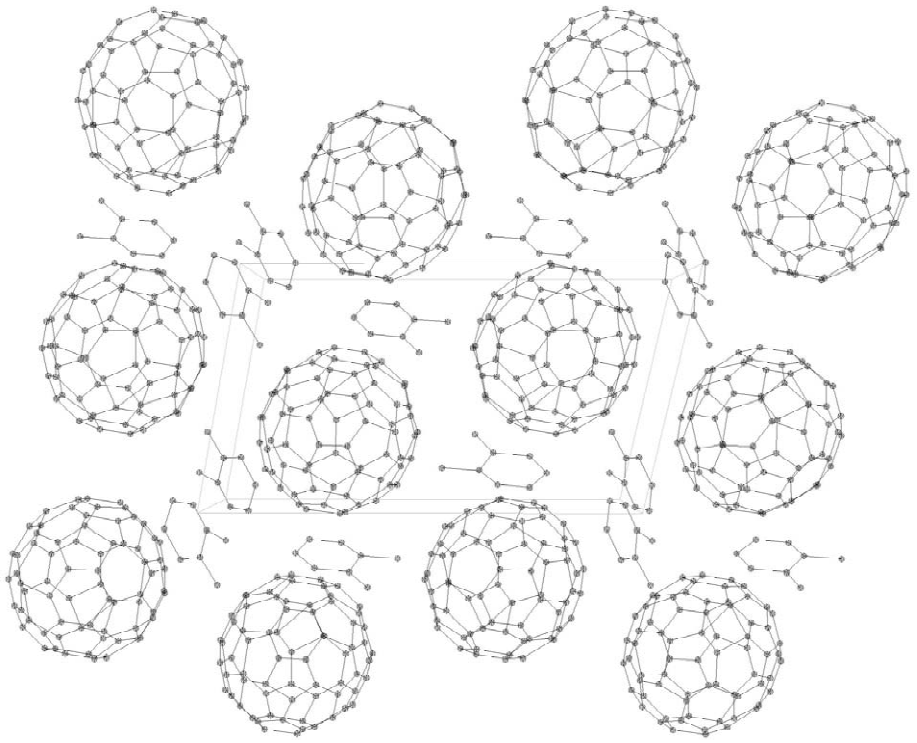

Fig. 5. Crystal structure of the solvate **5**.

Table 6
Thermodynamic properties, packing coefficients and dilution parameters for some C_{60} and C_{70} solvates

Solvate	$-\Delta V$ (Å^3)	d (dilution parameter)[a]	k (packing coefficient)[b]	$-\Delta S$ (1) (ΔS_{melt}) (J/mol K)	$-\Delta H$ (1) (ΔH_{melt}) (kJ/mol)
$C_{60}\cdot 2C_6H_5CH_3$	124(61) [30]	0.80	0.78	52 [1], (38.5)	15 [1], (6.8)
$C_{60}\cdot 2C_6H_5Br$	116(75) [20,31]	0.80	0.78	60 [20], (43.8)	21 [20], (10.6)
$C_{60}\cdot 2C_6H_5I$	125	0.83	0.78	65 [33], (40.4)	25 [33], (9.8)
$C_{60}\cdot 2CCl_4$	81(48) [23]	0.82	0.73	12 [34], (13.1)	5 [34], (3.3)
$C_{60}\cdot 2o\text{-}C_6H_4(CH_3)_2$	120	0.89	0.78	43 [1], (54.8)	15 [1], (13.6)
$C_{60}\cdot 2m\text{-}C_6H_4Br_2$	121	0.90	0.78	53 [11], (52)	20 [11], (14)
$C_{60}\cdot 3o\text{-}C_6H_4Br_2$	143	1.21	0.78	38 [11], (47)	13 [11], (13)
$C_{60}\cdot 2/3(m\text{-}C_6H_4Br_2)$	14	0.58	0.73	45 [11], (52)	22 [11], (14)
$C_{60}\cdot 2/3(m\text{-}C_6H_4Cl_2)$	8	0.58	0.72	47 [11], (51)	18 [11], (12.6)
$C_{60}\cdot 2/3(m\text{-}C_6H_4(CH_3)_2)$	17	0.58	0.73	50 [11], (51),	18 [11], (11.6)
$C_{60}\cdot 2/3(1,3,5\text{-}C_6H_5(CH_3)_3$	37	0.58	0.74	50 [11], (42)	24 [11], (9.5)
$C_{60}\cdot C_6H_5(CH_3)$	73(41) [30]	0.55	0.77	[c]	[c]
$C_{60}\cdot C_6H_5Cl$	66(36) [30]	0.55	0.77	[c]	[c]
$C_{70}\cdot 2o\text{-}C_6H_4(CH_3)_2$	162	0.81	0.78	31.5 [11], (55)	12 [1], (13.6)
$C_{60}\cdot n\text{-}C_8H_{18}$	86(24) [29]	0.71	0.75	39.5 [29], (95.5)	15 [29], (20.6)
$C_{60}\cdot n\text{-}C_7H_{16}$,	75(20) [29]	0.68	0.75	10 [29], (77.6),	3.5 [29], (14.6)

ΔV, change of volume in reaction (1) (in round brackets—in reaction (2)); molar volume of solid C_{60} is 710 Å^3.
ΔS (1), entropy change in reaction (1) per mole of a solvent (in round brackets—melting entropy of a pure solvent [35]).
ΔH (1), change of enthalpy in reaction (1) per mole of a solvent (in round brackets—enthalpy of melting of a pure solvent [35]).
[a] $d = \{V_{cell} - V(C_{60})\}/V(C_{60})$, $V(C_{60}) = 525$ A [3,32].
[b] $k = \{V_{mol}/V_{cell}\}$, where V_{mol} is the van der Waals volume of a formula unit.
[c] Enthalpies and entropies of reaction (1) were not determined.

Table 7
Comparison of experimental (calorimetry) and predicted lattice energies of C_{60} solvates

Solvate composition	Lattice energy (kJ/mol):			
	Experimental[a]	Calculated[b]		
		A	*B*	*C*
$C_{60}\cdot 2C_6H_5CH_3$	298	284		299
$C_{60}\cdot 2C_6H_5Br$	322	305		320
$C_{60}\cdot 2C_6H_5Cl$	303			300
$C_{60}\cdot 2m\text{-}C_6H_4Br_2$	341	332		349
$C_{60}\cdot 3o\text{-}C_6H_4Br_2$	403	400		416
$C_{70}\cdot 2o\text{-}C_6H_4Me_2$	329	299		327
$C_{60}\cdot C_6H_5CH_3$	233		216	222
$C_{60}\cdot C_6H_5Cl$	235		220	224
$C_{60}\cdot 2CCl_4$	265		273	308
'$C_{60}\cdot 2n\text{-}C_6H_{14}$'	≤254			261

[a] Calorimetric measurements corrected to 0 K (±10 kJ/mol).
[b] Model calculation with (*A*) cell dimensions and atomic coordinates fixed on experimental structure, (*B*) rigid body parameters optimized while cell dimensions fixed on experimental values (Table 4 for $C_6H_5CH_3$ and C_6H_5Cl; $a=b=10.10$, $c=10.75$ Å, $\alpha=\beta=90°$, $\gamma=120°$ [23] for CCl_4 solvates, respectively), and (*C*) full optimization.

C_{60} with the planar arene molecules and nearly spherical CCl_4 seems to be impossible for the alkanes due to their shape and linear dimensions. Larger molecules of aromatic solvents (*o*- and *m*-$C_6H_4Br_2$, *o*-xylene, chloronaphtalene, etc.) also do not fit this structure.

3.3. Lattice energies

In Tables 7 and 8, the observed lattice dimensions and the lattice energies of the solvates as derived from the calorimetric data are compared with those respective quantities predicted by PMC calculation.

Generally, the lattice energy of a fullerene solvate corresponds to the reaction

$$C_n \cdot rS(cr) = C_n(g) + rS(g) \quad \text{at } T = 0\text{ K}, n = 60 \text{ or } 70 \qquad (3)$$

The numbers in the second column ('experimental') of Table 7 were calculated from the experimental data on the reaction (1) [1,11] and from the enthalpies of evaporation of S [35] and the enthalpies of sublimation of C_{60} (170 kJ/mol [36]) and C_{70} (200 kJ/mol [37]) at $T=298$ K. The resulting enthalpies were then recalculated to 0 K. In neither case is a complete set of the heat capacities

Table 8
Deviations of the predicted structures from experimental[a]

Composition:						
Fullerene	C_{60}	C_{60}	C_{60}	C_{60}	C_{60}	C_{70}
Solvent	*m*-$C_6H_4Br_2$	PhMe	PhBr	PhCl	o-$C_6H_4Br_2$	$C_6H_4Me_2$
Content	1:2	1:2	1:2	1:2	1:3	1:2
Space group	*C2/m*	*C2/m*	*C2/m*	*C2/m*	$P2_1/c$	*P-1*
Cell-parameter deviations (%):						
$(a_{cal}-a_{exp})/a$	−2.0	−3.1	−3.3	−3.9	−1.3	−1.4
$(b_{cal}-b_{exp})/b$	−0.0	−1.0	−1.9	−0.2	−0.3	−2.6
$(c_{cal}-c_{exp})/c$	−2.5	−0.4	−0.0	−1.2	−3.5	−2.1
$(\alpha_{cal}-\alpha_{exp})/\alpha$	0.00	0.0	0.0	0.0	0.0	2.7
$(\beta_{cal}-\beta_{exp})/\beta$	0.31	1.7	1.6	1.1	−0.7	5.8
$(\gamma_{cal}-\gamma_{exp})/\gamma$	0.00	0.0	0.0	0.0	0.0	−1.8
Rigid-body parameters deviations:[b]						
Fullerene:						
T	0.00	0.00	0.00	0.00	0.00	0.18
ω	8.3	0.9	1.8	1.8	2.0	24.4
Solvent:[c]						
$\langle t\rangle$	0.04	0.08	0.07	0.87	0.16	0.21
$\langle\omega\rangle$	5.5	2.0	1.1	1.9	2.2	6.1

[a] Experimental parameters of $C_{60}\cdot 2m\text{-}C_6H_4Br_2$; $C_{60}\cdot 2C_6H_5CH_3$; $C_{60}\cdot 3o\text{-}C_6H_5Br_2$ and $C_{70}\cdot 2m\text{-}C_6H_4CH_3$ were determined in the present study (see Table 1); for $C_{60}\cdot 2C_6H_5Br$ they were taken from Ref. [19]; for the chlorobenzene solvate $C_{60}\cdot 2C_6H_5Cl$, whose experimental structure is totally unknown, the deviations given refer to the experimental bromobenzene solvate $C_{60}\cdot 2C_6H_5Br$ [20].
[b] t (Å) is the net translational molecule displacement from experimental to predicted position; ω (deg) is the turn angle required to align the predicted orientation of the molecule with the experimental one.
[c] Averaged over the two or three solvent molecules.

necessary for such a recalculation available. It was assumed, that the enthalpy of the reaction (2) is temperature independent from 298 to 0 K; the changes of sublimation enthalpies are $\Delta\Delta H$ (C_{60}, sc, sublimation, 298 K→0 K)= 7 kJ/mol [37] and $\Delta\Delta H$ (C_{70}, sublimation, 298 K→0 K)=5 kJ/mol [37], and the changes of sublimation enthalpy $\Delta\Delta H$ (S, sublimation, 298 K→0 K)=7 kJ/mol [38] are roughly the same for all the solvents S in Table 7.

The PMC calculations were performed in two different ways. First, whenever a full crystal structure was available (i.e., **1a**, **3**, **4, 5** and $C_{60}\cdot 2C_6H_5Br$ [20] the energies were calculated with experimental unit cell parameters and atomic coordinates without previous minimization (see column A in Table 7). Second, optimal crystal packings (formally equilibrium structures at absolute zero temperature) were calculated by minimization of the lattice energy with respect to the lattice constants and rigid body parameters of the fullerene and solvent molecules. The known cell dimensions and space group were taken as a guide to select initial structures in the minimization. The final minimized energies are presented in the column C of Table 7.

For the geometrically similar monoclinic structures of $C_{60}\cdot 2C_6H_5Br$ and $C_{60}\cdot 2C_6H_5CH_3$ the energy minimization was performed starting from the experimental (see Table 1) as well as from a number of randomly chosen starting structures. The observed *C2/m* symmetry was not maintained except for the centering translation. The lowest energy minima found with various starting models were invariably the same crystal structure in very close agreement with the experimental structure. Remarkably, the resulting lattice geometry and space group were exactly identical with the experimentally observed ones, including the site symmetries of both the C_{60} and the solvent molecules.

For the triclinic $C_{70}\cdot 2o\text{-}C_6H_4Me_2$ and monoclinic $C_{60}\cdot 3o\text{-}C_6H_4Br_2$ solvates, the energy minimizations were performed starting from two experimental structures only (Table 3). The observed symmetry was maintained during minimization: this suggested three sets of six rigid body parameters in the first structure (one for C_{70} and two for solvent in general position) and four sets for the second (one for C_{60} and three for solvent).

The deviations of the optimal structural parameters from experimental ones for the four solvates **1a**, **3, 4a,** and **5** are reported in Table 8.

The experimental crystal structure of the $C_{60}\cdot 2C_6H_5Cl$ solvate is not yet available. This complex however was clearly identified by DSC [33]. In this work, we propose its crystal structure to be similar to the monoclinic structures observed for the present 1:2 bromobenzene and toluene solvates in order to further model its optimal geometry and energy with the above approach. This enables us to get a theoretical value of the lattice energy (column C) of yet unknown structure which can be compared with the calorimetry experiment. The energy minimization were thus performed as above with the bromobenzene and toluene solvates, their coordinates were used as staring ones in the chlorobenzene analogue. The resulting optimal parameters of the crystal structure are again in Table 8 in terms of deviations from the bromobenzene solvate.

With this approach, we turn now to the $C_{60}\cdot 2CCl_4$ solvate, whose crystal is known to be of hexagonal symmetry, space group *P6/mmm* [23], and is similar in packing motif to monoclinic solvates $C_{60}\cdot 2C_6H_5X$ (X= CH_3, Br, I) described above. In the case of $C_{60}\cdot 2CCl_4$, energy minimization was performed by varying both six lattice constants and rigid-body parameters within P1 space group. For completeness of Table 7, fixed-cell minimization was also made afterwards starting from the fully optimized structure (Column B).

The monoclinic cell dimensions of the $C_{60}\cdot C_6H_5Me$ (**1b**) in the present work are similar to those of the orthorhombic modification of the same compound $C_{60}\cdot C_6H_5Me$ (**1c**) reported earlier [39]. The structural model of that phase has been derived by energy minimization and confirmed by the low *R*-factor calculated from the powder spectrum. In this study we used the structure of (**1c**) as the initial model to minimize energy minimization in the *Cc* space group for **1b** and for **6** ($C_{60}\cdot C_6H_5Cl$) structures. Two values of lattice energies for **1b** and **6** in the Table 7 correspond to the lowest minimum of the lattice energy found (column C) and the minimum lattice energy with the unit cell parameters fixed at experimental values (column B).

A comparison of observed and calculated energies (Table 7) demonstrates their common trend along the present series of solvates. In particular, the energies of the fully optimized structures reproduce the calorimetric results corrected to 0 K fairly well.

The $C_{60}\cdot 2CCl_4$ solvate is an outlier from the trend. Its minimized energy based on the optimimal structure (column C) was found to be about 16% more negative than the experimental energy, while the *c*-axis length dropped to 9.9 Å as compared to 10.75 Å observed. This disagreement can be explained by the instability of the perfectly hexagonal packing at absolute zero, while at ambient conditions it is stabilized by orientational motion and disorder of nearly spherical molecules.

In Table 8, the parameters of the optimized structures are compared with the X-ray single crystal data (Table 1) in terms of deviations of the former with respect to latter. As is seen from the table, the simulated crystal structures with the minimum energy at 0 K ('optimal structures') are usually similar to the experimental ones, observed at higher temperatures. In case of $C_{60}\cdot 2C_6H_5CH_3$ and $C_{60}\cdot 2C_6H_5Br$ the positional and orientational parameters for C_{60} and solvent molecules for calculated and observed structures are remarkably close. For $C_{60}\cdot 2m\text{-}C_6H_4Br_2$ the orientation of fullerene moiety is slightly different in comparison with experimental one. The calculated unit cell parameters differ from observed ones by 0.23 Å for lattice

periods and 1.8° for the angles on the average; more often the *a*, *b*, *c* parameters are lowered in comparison with experiment. The shortest intermolecular atom–atom distances for simulated structures are close to the sum of the van der Waals radii although they are slightly shorter than the distances experimentally determined.

The structures of $C_{60}\cdot 2m\text{-}C_6H_4Br_2$ and $C_{60}\cdot 3o\text{-}C_6H_4Br_2$ possess a notable feature: very short Br···Br contacts down to 3.4 Å have been observed in the experiment. The shortened Br···Br contacts were reproduced in our calculations, although these contacts were slightly longer compared to experiment. The remaining contacts were found to be shorter generally by 0.1–0.2 Å in comparison with experiment.

The prediction of the exothermicity of the reactions (1) is a challenging problem. PMC was used to calculate the lattice energy of the hypothetical monoclinic crystal of $C_{60}\cdot 2C_6H_{14}$ solvate which was not yet obtained by experiment, probably because the C_6H_{14} molecule shape and dimensions do not fit in this type of lattice (Fig. 1, see above). The optimal structure of $C_{60}\cdot 2C_6H_{14}$ has a lattice energy of 261 kJ/mol which corresponds to a nearly zero (−7 kJ/mol) enthalpy of the reaction (1) at 0 K. For the existing solvates of this type, $C_{60}\cdot 2C_6H_5Br$ and $C_{60}\cdot 2C_6H_5CH_3$, the experimental enthalpies of reaction (1) are −42 and −30 kJ/mol [1], respectively, while the ones, based on the optimal PMC lattice energies are −44 and −31 kJ/mol, respectively. It may be stated that PMC is able to reproduce the difference in thermal stability of the (1:2) solvates with arenes and of the hypothetical $C_{60}\cdot 2C_6H_{14}$ solvate, and to explain the low stability of the latter.

Acknowledgements

Authors are grateful to Professor M.Yu. Antipin for his help in arranging of the single crystal X-ray study. The work was supported by RFBR (grants 99-03-32810 and 00-03-32097).

References

[1] Korobov MV, Mirakian AL, Avramenko NV, Ollofson G, Ruoff R, Smith AL. Calorimetric studies of solvates of C_{60} and C_{70} with aromatic solvents. J Phys Chem B 1999;103(8):1339–46.

[2] Iwasa Y, Tanoue K, Mitani T, Izuoka A, Sugawara T, Yagi T. High yield selective synthesis of C_{60} dimers. Chem Commun 1998:1411–2.

[3] Meidine MF, Hitchcock PB, Kroto HW, Taylor R, Walton DRM. Single-crystal X-ray structure of benzene-solvated C_{60}. J Chem Soc Chem Commun 1992:1534–7.

[4] Balch AL, Lee JW, Noll BC, Olmstead MM. Disorder in a crystalline form of buckminsterfullerene: $C_{60}\cdot 4C_6H_6$. J Chem Soc Chem Commun 1993:56–8

[5] Ramm M, Luger P, Zobel D, Duczek W, Boyens JCA. Static disorder in hexagonal crystal structures of C_{60} at 100 K and 20 K. Cryst Res Technol 1996;31:43–53.

[6] Boyens JCA, Ramm M, Zobel D, Luger P. Static disorder and packing in two orthorhombic crystal structures of fullerene inclusion compounds. S Afr J Chem 1997;50(1):28–33.

[7] Gorun SM, Creegan KM, Sherwood RD, Cox DM, Day VW, Day CS et al. Solvated C_{60} and C_{60}/C_{70} and the low-resolution single crystal X-ray structure of C_{60}. J Chem Soc Chem Commun 1991:1556–8.

[8] Gritsenko VV, Dyachenko OA, Kushch ND, Spitsina NG, Yagubskii EB, Avramenko NV et al. C_{60} solvate with trichloroethylene, C_{60},C_2HCl_3. Russ Chem Bull 1994;43:1183–5.

[9] Talyzin AV, Zaitseva NV, Syrnicov PP. Growth of C70 crystals from benzene solutions. In: Kadish K, Ruoff R, editors, Recent advances in the chemistry and physics of fullerenes and related materials, vol. 4, NJ: Electrochemical Society; 1997, pp. 551–66.

[10] Agafonov V, Ceolin R, Andre D, de Bruijn J, Gonthier-Vassal A, Szwarc H et al. Fullerene C70, toluene 1:1 solvate: structural and thermodynamic evidences. Chem Phys Lett 1993;208:68–72.

[11] Avramenko NV, Stukalin EB, Korobov MV, Neretin IS, Slovokhotov YuL. Binary systems of C_{60} with positional isomers 1,2- and 1,3-$C_6H_4Br_2$. Thermochim Acta 2001;370:21–8.

[12] SHELXTL, an integrated system for solving, refining and displaying crystal structures from diffraction data, Ver. 5.10., Bruker Analytical X-ray Systems, Madison, WI, USA, 1997.

[13] Werner P-E, Eriksson L, Westdahl M. TREOR, a semi-exhaustive trial-and-error powder indexing program for all symmetries. J Appl Crystallogr 1985;18(5):367–70.

[14] Kitaigorodskii AI. In: Molecular crystals and molecules, New York: Academic Press; 1973.

[15] Dzyabchenko AV, Agafonov V, Davydov VA. A theoretical study of the pressure-induced dimerization of C_{60} fullerene. J Phys Chem A 1999;103(15):2812–20.

[16] Dzyabchenko AV. In: PMC (Version 2002). A program to predict packings of molecules in crystals. User's guide, Moscow: Karpov Institute of Physical Chemistry; 2002.

[17] Nemethy G, Scheraga HA. Intermolecular potentials from crystal data. 5. Determination of empirical potentials for O–H···O hydrogen bonds from packing configurations and lattice energies of polyhydric alcohols. J Phys Chem 1977;81(9):928–31.

[18] Soldatov AV, Roth G, Dzyabchenko A, Johnels D, Lebedkin S, Meingast C et al. Topochemical polymerization of C-70 controlled by monomer crystal packing. Science 2001;293:680–3.

[19] Dzyabchenko AV. Calculation of optimal packings of molecules in organic crystals in atom–atom approximation. Moscow, Karpov Institute of Physical Chemistry, PhD thesis, 1980.

[20] Korobov MV, Mirakian AL, Avramenko NV, Valeev EF, Neretin IS, Slovokhotov YuL et al. C60·bromobenzene solvate: Crystallographic and Thermochemical Studies and their relationship to C60 solubility in bromobenzene. J Phys Chem B 1998;102(19):3712–7.

[21] Crane JD, Hitchcock PB, Kroto HW, Taylor R, Walton DRM.

Preparation and characterization of C_{60}(ferrocenne)$_2$. Chem Commun 1992:1764–5.

[22] Konarev DV, Valeev EF, Slovokhotov YuL, Lyubovskaya RN. A series of a new molecular complexes $C_{60}(S_4N_4)_{2-x}(C_6H_6)_x$ synthesis, X-ray study of crystal structure and structural disorder. J Phys Chem Solids 1997;58(11):1865–7.

[23] Ceolin R, Agafonov V, Andre D, Dworkin A, Szwarc H, Dugue J et al. Fullerene C_{60},2CCl_4 *solvate*. A solid-state study. Chem Phys Lett 1993;208:259–62.

[24] Jansen M, Waidmann G. Synthesis and characterization of the fullerene co-crystals $C_{60}\cdot 12C_6H_{12}$, $C_{70}\cdot 12C_6H_{12}$, $C_{60}\cdot 12CCl_4$, $C_{60}\cdot 2CHBr_3$, $C_{60}\cdot 2CHCl_3$, $C_{60}\cdot 2H_2CCl_2$. Z Anorg Allg Chem 1995;621:14–8.

[25] Douthwaite RE, Green MLH, Heyes SJ, Rossinsky MJ, Turner JFC. Synthesis and characterisation of the inclusion complex $\{(P_4)_2C_{60}\}$. J Chem Soc Chem Commun 1994:1367–8.

[26] Roth G, Adelmann P. Preparation and crystal structure of $C_{60}S_{16}$. Appl Phys A 1993;56:169–74.

[27] Geiser U, Kalyan Kumar S, Savall BM, Harried SS, Carlson KD, Mobley PR et al. Discrete layers of ordered C_{60} molecules in the cocrystal $C_{60}\cdot CH_2I_2\cdot C_6H_6$: synthesis, crystal structure, and ^{13}C NMR properties. Chem Mater 1992;4:1077–82.

[28] Birkett PR, Christides C, Hitchcock PB, Kroto HW, Prassides K, Taylor R et al. Preparation and single-crystal structure determination of the solvated intercalate C_{60},I_2,toluene. J Chem Soc Perkin Trans 1993;2:1407–8.

[29] Ceolin R, Michaud F, Toscani S, Agafonov V, Tamarit J, Dworkin A et al. Crystals of C_{60} solvates. In: Kadish K, Ruoff R, editors, Recent advances in the chemistry and physics of fullerenes and related materials, vol. 5, NJ: Electrochemical Society; 1997, pp. 373–81.

[30] Anderson M, Bosio L, Bruneaux-Poulle J, Fourme R. Toluene: structure crystalline et moleculaire de la variete stable α et etat amorphe. J Chim Phys 1977;74(1):69–73.

[31] Clavagneta-Plajs N. These Doct., Troisieme Cycle, Orsay 1970.

[32] Slovokhotov YuL, Moskaleva IV, Shil'nikov VI, Valeev EF, Novikov YN, Yanovsky AI et al. Molecular and crystal structures of C_{60} derivatives: CSD statistics and theoretical modeling. Mol Mater 1996;8:117–24.

[33] Marcus Y, Smith A, Korobov M, Mirakyan A, Avramenko NA, Stukalin EB. Solubility of a C_{60} fullerene. J Phys Chem B 2001;105(13):2499–506.

[34] Barrio M, Lopez D, Tamarit J, Szwarc H, Toscani S, Ceolin R. C_{60}-CCl_4 phase diagram: polythermal behaviour of solvates C_{60},12CCl_4 and C_{60},2CCl_4 Chem. Phys Lett 1996;260:78–81.

[35] Lide DR, editor, CRC handbook of chemistry and physics, 77th ed, New York, London, Tokyo: CRC Press; 1996.

[36] Bohme D, Boltalina O, Hvelplund P. Fullerenes and fullerene ions in the gas phase. In: Kadish K, Ruoff R, editors, Fullerenes, New York: Wiley; 2000, pp. 481–530.

[37] Diky VV, Kabo GYa. Thermodynamic properties of C_{60} and C_{70} fullerenes. Uspechi Kchimii 2000;69(2):95–105, (In Russian).

[38] http://webbook.nist.gov.

[39] Dzyabchenko AV, Agafonov V, Ceolin R. Crystal structure of the 1:1 C_{60}-toluene solvate found by lattice energy minimization and confirmed by X-ray powder diffraction. Book of abstracts, IWFAC 2001. St. Petersburg, Russia 2001:236.